From Myoglobin to Heme-Copper Oxidase: Design and Engineering of a Cu_B Center into Sperm Whale Myoglobin

Jeffrey A. Sigman, Brian C. Kwok, and Yi Lu*

Contribution from the Department of Chemistry, University of Illinois at Urbana−Champaign, Urbana, Illinois 61801

Received May 3, 2000

Abstract: Myoglobins (Mb) are small globular heme proteins that serve as O_2 carriers. Heme-copper oxidases (HCOs) are large membrane-bound proteins that catalyze proton-coupled reduction of O_2 to water. Mb contains a single heme center, while HCOs contain a high-spin heme-Cu_B dinuclear center, a low-spin heme center, and in certain subclasses of HCO enzymes such as cytochrome *c* oxidases (C*c*O) a dinuclear copper center called Cu_A. While Mb is one of the most well-characterized proteins, many questions about the structure and function of HCOs, such as the role of the Cu_B center, the origin of spin coupling between Cu_B and heme, and the exact nature of the reaction intermediates, remain to be fully understood. We report here the design and engineering of a copper-binding site in sperm whale myoglobin (swMb) based on structural comparison and computer modeling of swMb and C*c*O. UV−vis studies of the resting state of the designed protein swMb-((L29H, F43H) (called Cu_BMb) suggest that a single copper-binding site is created in swMb. UV−vis, elemental analysis, and EPR studies of the cyanide-bound Cu_BMb indicate that a spin-coupled, CN^--bridged Cu_B-heme center is formed in the designed model protein, as in the native HCOs. Parallel spectroscopic studies with Zn(II) in the place of Cu(II) further support the conclusion. The study also reveals that the presence of Cu(II) and Ag(I) (as a Cu(I) mimic) increased the affinity of heme for diatomic ligands such as CN^- and O_2. This study shows that it is possible to design and engineer metal-binding sites in proteins with little sequence and structural homology. The resulting designed protein, free from other chromophores, is more amendable to biochemical and biophysical studies. Spectroscopy studies of the designed protein indicate that the Cu_B center plays an important role in HCO structure and function.

Heme-copper oxidases (HCOs)[1] are a superfamily of terminal oxidases in the respiratory chains of both eukaryotic mitochondria and bacteria.[2−6] They are metalloenzymes containing a low-spin heme center and a high-spin heme-Cu_B dinuclear center (Figure 1). In addition, cytochrome *c* oxidases contain another dinuclear copper center called Cu_A.[7] Heme-copper oxidases catalyze the reduction of molecular oxygen to water and harness the free energy from this reaction to pump protons across the cytoplasmic or mitochondrial membranes. The resulting proton concentration and electrostatic potential gradient generated across the membranes drive the synthesis of ATP, the universal energy source for many cellular processes. Heme-copper oxidases catalyze 90% of molecular oxygen reduction in the biosphere.[8] HCO deficiencies or naturally occurring mutations have been linked to Alzheimer's disease,[9] Leigh syndrome,[10] and aging.[11] Therefore, understanding the structure and function of this enzyme superfamily has been the focus of intense biochemical,[12−15] spectroscopic,[16−23] X-ray crystallographic,[24−28] and biomimetic modeling studies.[29−36]

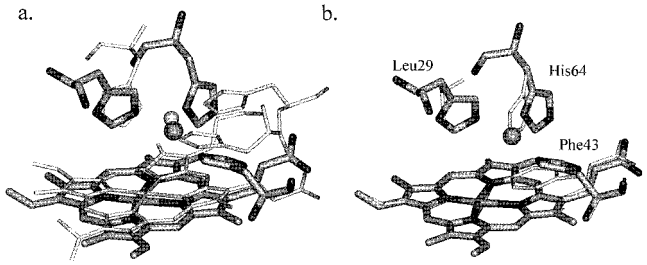

Figure 1. (a) Overlay of heme-copper centers of a computer model of Cu_BMb (thick) from the present work and a crystal structure of bovine heart C*c*O[26] (thin). (b) Overlay of active sites of a computer model of Cu_BMb (thick) from the present work and a crystal structure of WTswMb[56] (thin).

* Corresponding author. Phone: (217) 333-2619. Fax: (217) 333-2685. E-mail: yi-lu@uiuc.edu.

(1) Abbreviations: HCO, heme-copper oxidase; C*c*O, cytochrome *c* oxidase; Mb, myoglobin; swMb, sperm whale myoglobin; Cu_BMb, swMb-(L29H, F43H).

(2) Babcock, G. T.; Wikström, M. *Nature (London)* **1992**, *356*, 301.
(3) Garcia-Horsman, J. A.; Barquera, B.; Rumbley, J.; Ma, J.; Gennis, R. B. *J. Bacteriol.* **1994**, *176*, 5587.
(4) Ferguson-Miller, S.; Babcock, G. T. *Chem. Rev.* **1996**, *96*, 2889.
(5) Michel, H.; Behr, J.; Harrenga, A.; Kannt, A. *Annu. Rev. Biophys. Biomol. Struct.* **1998**, *27*, 329.
(6) Poulos, T. L.; Li, H.; Raman, C. S. *Curr. Opin. Chem. Biol.* **1999**, *3*, 131.
(7) Beinert, H. *Eur. J. Biochem.* **1997**, *245*, 521.
(8) Slater, E. C.; van Gelder, B. F.; Minnaert, K. In *Oxidases and related redox systems*; King, T. E., Mason, H. S., Morrison, M., Eds.; John Wiley & Sons: New York, 1965; p 667.
(9) Davis, R. E.; Miller, S.; Herrnstadt, C.; Ghosh, S. S.; Fahy, E.; Shinobu, L. A.; Galasko, D.; Thal, L. J.; Beal, M. F.; Howell, N.; Parker, W. D., Jr. *Proc. Natl. Acad. Sci. U.S.A.* **1997**, *94*, 4526.
(10) Zhu, Z.; Yao, J.; Johns, T.; Fu, K.; De Bie, I.; Macmillan, C.; Cuthbert, A. P.; Newbold, R. F.; Wang, J.-c.; Chevrette, M.; Brown, G. K.; Brown, R. M.; Shoubridge, E. A. *Nat. Genet.* **1998**, *20*, 337.
(11) Paradies, G.; Ruggiero, F. M.; Petrosillo, G.; Quagliariello, E. *FEBS Lett.* **1997**, *406*, 136.
(12) Thomas, J. W.; Calhoun, M. W.; Lemieux, L. J.; Puustinen, A.; Wikström, M.; Alben, J. O.; Gennis, R. B. *Biochemistry* **1994**, *33*, 13013.
(13) Calhoun, M. W.; Hill, J. J.; Lemieux, L. J.; Ingledew, W. J.; Alben, J. O.; Gennis, R. B. *Biochemistry* **1993**, *32*, 11524.

10.1021/ja0015343 CCC: $19.00
Published on Web 08/09/2000

A main goal of the current research is to understand the reaction mechanism of dioxygen reduction at the molecular level, including the geometric and electronic structure of the resting state enzyme as well as its reaction intermediates. While tremendous progress has been made in the study of heme-copper oxidases,[2−6] the role of Cu_B, the origin of spin coupling between Cu_B and heme, the exact nature of the reaction intermediates, and thus the reaction mechanism remain to be fully understood.[4,37,38] Biochemically it has been difficult to obtain HCOs, which are large (MW ≈ 200 000), membrane-bound proteins, in a single homogeneous form. Spectroscopic signals from the heme-copper center are often masked by signals from other metal-binding sites. For example, both UV−vis and MCD spectra of HCOs are dominated by the low-spin heme center. Therefore, to obtain information about the heme-copper center, particularly the information about the reaction intermediates, difference spectra had to be used.

Myoglobin (Mb) is a small (MW ≈ 17 000) globular heme protein that serves as an O_2 carrier in many biological systems.[39,40] The system for construction, purification, and characterization of myoglobins and their various mutant forms is well established.[41−45] Myoglobin binds O_2 reversibly, while HCOs binds O_2 *and* reduces it to H_2O. Despite this difference, the oxy derivative of HCO has been compared to the oxy derivative of Mb.[46,47] An interesting question is what factors make HCOs reduce O_2 to H_2O. A still further interesting question is how to covert Mb from a reversible O_2 binder to an O_2 activator as the HCOs.

We are interested in investigating the role of the Cu_B center in the catalytic active site of HCOs by design and engineering of the Cu_B center into heme proteins such as cytochrome *c* peroxidase[48] and myoglobin. Design and engineering of a Cu_B center into Mb will allow a direct comparison of Mb and HCO in the same protein framework. It can help answer a particularly interesting question of the role of Cu_B in heme-copper oxidase function. Since Mb can be obtained in a single homogeneous form and the engineered heme-copper center in Mb will be free of other chromophores, the resulting HCO model proteins will be quite amenable to spectroscopic studies. Finally, the role of copper ions can be further elucidated by replacing the copper ions with other divalent metal ions such as Zn(II) in the model proteins, a task not yet achieved in the native HCO systems.

Design and engineering of metal-binding sites in proteins is another exciting area of research.[49−51] Despite recent progress,[48,52−55] much remains to be understood about how to design and construct metal-binding sites in proteins, particularly when no sequence or structure homology is found. Therefore, design and engineering of a Cu_B center in Mb will not only help elucidate the structure and function of heme-copper oxidases, but also contribute to the understanding of *de novo* metalloprotein design.

Here we present the design and engineering of a copper-binding site in sperm whale myoglobin. UV−vis and EPR spectroscopic characterization of the resting state of the redesigned protein swMb(L29H, F43H) (called Cu_BMb hereafter), as well as the different metal ion and ligand derivatives, strongly suggests that a Cu_B center is created in swMb and the protein model closely mimics the Cu_B-heme center in heme-copper oxidases. More importantly, this model protein allowed us to provide direct evidence for the importance of Cu_B centers in the structure and function of heme-copper oxidases.

Materials and Methods

Computer Modeling. Molecular modeling of the copper site in Mb was performed on a Silicon Graphics Irix^2 computer utilizing Quanta97

(14) Cheesman, M. R.; Watmough, N. J.; Pires, C. A.; Turner, R.; Brittain, T.; Gennis, R. B.; Greenwood, C.; Thomson, A. J. *Biochem. J.* **1993**, *289*, 709.
(15) Shapleigh, J. P.; Hosler, J. P.; Tecklenburg, M. M. J.; Kim, Y.; Babcock, G. T.; Gennis, R. B.; Ferguson-Miller, S. *Proc. Natl. Acad. Sci. U.S.A.* **1992**, *89*, 4786.
(16) Thomson, A. J.; Greenwood, C.; Gadsby, P. M. A.; Peterson, J.; Eglinton, D. G.; Hill, B. C.; Nicholls, P. *J. Inorg. Biochem.* **1985**, *23*, 187.
(17) Martin, C. T.; Scholes, C. P.; Chan, S. I. *J. Biol. Chem.* **1985**, *260*, 2857.
(18) Watmough, N. J.; Cheesman, M. R.; Gennis, R. B.; Greenwood, C.; Thomson, A. J. *FEBS Lett.* **1993**, *319*, 151.
(19) Oertling, W. A.; Surerus, K. K.; Einarsdottir, O.; Fee, J. A.; Dyer, R. B.; Woodruff, W. H. *Biochemistry* **1994**, *33*, 3128.
(20) Hosler, J. P.; Kim, Y.; Shapleigh, J.; Gennis, R.; Alben, J.; Ferguson-Miller, S.; Babcock, G. *J. Am. Chem. Soc.* **1994**, *116*, 5515.
(21) Fann, Y. C.; Ahmed, I.; Blackburn, N. J.; Boswell, J. S.; Verkhovskaya, M. L.; Hoffman, B. M.; Wikström, M. *Biochemistry* **1995**, *34*, 10245.
(22) Fox, S.; Nanthakumar, A.; Wikström, M.; Karlin, K. D.; Blackburn, N. J. *J. Am. Chem. Soc.* **1996**, *118*, 24.
(23) Musser, S. M.; Fann, Y.-C.; Gurbiel, R. J.; Hoffman, B. M.; Chan, S. I. *J. Biol. Chem.* **1997**, *272*, 203.
(24) Tsukihara, T.; Aoyama, H.; Yamashita, E.; Tomizaki, T.; Yamaguchi, H.; Shinzawa-Itoh, K.; Nakashima, R.; Yaono, R.; Yoshikawa, S. *Science (Washington, D.C.)* **1995**, *269*, 1069.
(25) Iwata, S.; Ostermeier, C.; Ludwig, B.; Michel, H. *Nature (London)* **1995**, *376*, 660.
(26) Tsukihara, T.; Aoyama, H.; Yamashita, E.; Tomizaki, T.; Yamaguchi, H.; Shinzawa-Itoh, K.; Nakashima, R.; Yaono, R.; Yoshikawa, S. *Science (Washington, D.C.)* **1996**, *272*, 1136.
(27) Ostermeier, C.; Harrenga, A.; Ermler, U.; Michel, H. *Proc. Natl. Acad. Sci. U.S.A.* **1997**, *94*, 10547.
(28) Yoshikawa, S.; Shinzawa-itoh, K.; Nakashima, R.; Yaono, R.; Yamashita, E.; Inoue, N.; Yao, M.; Fei, M. J.; Libeu, C. P.; Mizushima, T.; Yamaguchi, H.; Tomizaki, T.; Tsukihara, T. *Science (Washington, D.C.)* **1998**, *280*, 1723.
(29) Nanthakumar, A.; Nasir, M. S.; Karlin, K. D.; Ravi, N.; Huynh Boi, H. *J. Am. Chem. Soc.* **1992**, *114*, 6564.
(30) Lee, S. C.; Holm, R. H. *J. Am. Chem. Soc.* **1993**, *115*, 5833.
(31) Collman, J. P.; Herrmann, P. C.; Boitrel, B.; Zhang, X.; Eberspacher, T. A.; Fu, L.; Wang, J.; Rousseau, D. L.; Williams, E. R. *J. Am. Chem. Soc.* **1994**, *116*, 9783.
(32) Casella, L.; Monzani, E.; Gullotti, M.; Gliubich, F.; De Gioia, L. *J. Chem. Soc., Dalton Trans.* **1994**, 3203.
(33) Nanthakumar, A.; Fox, S.; Murthy, N. N.; Karlin, K. D. *J. Am. Chem. Soc.* **1997**, *119*, 3898.
(34) Baeg, J.-O.; Holm, R. H. *Chem. Commun. (Cambridge)* **1998**, 571.
(35) Sasaki, T.; Nakamura, N.; Naruta, Y. *Chem. Lett.* **1998**, 351.
(36) Collman, J. P.; Rapta, M.; Broering, M.; Raptova, L.; Schwenninger, R.; Boitrel, B.; Fu, L.; L'Her, M. *J. Am. Chem. Soc.* **1999**, *121*, 1387.
(37) Gennis, R. B. *Proc. Natl. Acad. Sci. U.S.A.* **1998**, *95*, 12747.
(38) Proshlyakov, D. A.; Pressler, M. A.; Babcock, G. T. *Proc. Natl. Acad. Sci. U.S.A.* **1998**, *95*, 8020.
(39) Antonini, E.; Brunori, M. *Hemoglobin and Myoglobin in Their Reactions with Ligands*; North-Holland: London, 1971.
(40) Springer, B. A.; Sligar, S. G.; Olson, J. S.; Phillips, G. N., Jr. *Chem. Rev. (Washington, D.C.)* **1994**, *94*, 699.
(41) Springer, B. A.; Sligar, S. G. *Proc. Natl. Acad. Sci. U.S.A.* **1987**, *84*, 8961.
(42) Adachi, S.; Nagano, S.; Ishimori, K.; Watanabe, Y.; Morishima, I.; Egawa, T.; Kitagawa, T.; Makino, R. *Biochemistry* **1993**, *32*, 241.
(43) Christian, J. F.; Unno, M.; Sage, J. T.; Champion, P. M.; Chien, E.; Sligar, S. G. *Biochemistry* **1997**, *36*, 11198.
(44) Decatur, S. M.; Belcher, K. L.; Rickert, P. K.; Franzen, S.; Boxer, S. G. *Biochemistry* **1999**, *38*, 11086.
(45) Murakami, T.; Morishima, I.; Matsui, T.; Ozaki, S.-i.; Hara, I.; Yang, H.-J.; Watanabe, Y. *J. Am. Chem. Soc.* **1999**, *121*, 2007.
(46) Watmough, N. J.; Cheesman, M. R.; Butler, C. S.; Little, R. H.; Greenwood, C.; Thomson, A. J. *J. Bioenerg. Biomembr.* **1998**, *30*, 55.
(47) MacMillan, F.; Kannt, A.; Behr, J.; Prisner, T.; Michel, H. *Biochemistry* **1999**, *38*, 9179.
(48) Sigman, J. A.; Kwok, B. C.; Gengenbach, A.; Lu, Y. *J. Am. Chem. Soc.* **1999**, *121*, 8949.
(49) Regan, L. *Trends Biochem. Sci.* **1995**, *20*, 280.
(50) Hellinga, H. W. *Curr. Opin. Biotechnol.* **1996**, *7*, 437.
(51) Lu, Y.; Valentine, J. S. *Curr. Opin. Struct. Biol.* **1997**, *7*, 495.
(52) Farinas, E.; Regan, L. *Protein Sci.* **1998**, *7*, 1939.
(53) Pinto, A. L.; Hellinga, H. W.; Caradonna, J. P. *Proc. Natl. Acad. Sci. U.S.A.* **1997**, *94*, 5562.
(54) Hellinga, H. W. *J. Am. Chem. Soc.* **1998**, *120*, 10055.
(55) Yeung, B. K. S.; Wang, X. T.; Sigman, J. A.; Petillo, P. A.; Lu, Y. *Chem., Biol.* **1997**, *4*, 215.

(Molecular Simulations Inc.). The coordinates for swMb[56] and cytochrome *c* oxidase (C*c*O) from either bovine heart[26] or *Paracoccus denitrificans*[25] were obtained from the Protein Data Bank. The swMb structure was minimized using the Steepest Descents method in CHARMm for 1000 steps. The RTF files for heme and amino acids with polar hydrogen atoms were used as constraints. This procedure removed close contacts and provided a basis for comparison to the energy of the mutant protein structures. Once the structure was minimized, the distal heme pocket in swMb was compared to C*c*O and evaluated for possible mutation sites. The initial strategy was to design a Cu(II) binding site by using residues with side chains already oriented into the heme pocket to avoid large structural modifications (Figure 1).

Several residues in the distal pocket of swMb may serve as ligands for a Cu_B-binding site. Of the several residues oriented into the distal pocket, Leu29 and Phe43 were chosen and mutated to histidines. His64, in the distal pocket, was already in approximately the right position to serve as a ligand to the copper ion. A copper ion was inserted into the structure, and 500 kcal constraints were put on the copper ion and coordinating histidine nitrogen atoms. The minimized structure was again compared to the native C*c*O.

Construction, Expression, and Purification of Engineered Proteins. All site-directed mutagenesis experiments were performed using the QuikChange Site Directed Mutagenesis Kit (Stratagene, CA). The Leu29His and Phe43His mutations in the swMb gene of pMbt7-7 were confirmed by DNA sequencing at the Biotechnology Center in the University of Illinois. The published procedure for the purification of sperm whale Mb[41] was used for the preparation of this protein with the following changes. The BL-21(DE3) bacterial pellet containing the protein was resuspended in 20 mM Tris pH 8 containing 1 mM EDTA, 0.5 mM DTT, 1 mM PMSF, 40 units/mL DNAaseI, and 20 units/mL RNAaseI. The cells were lysed by passage through a French press cell. The crude lysate was filtered and purified through a DEAE CL-6B anion-exchange column. The myoglobin was collected, concentrated, and then loaded onto a gel filtration column equilibrated with 100 mM KH_2PO_4, pH 7. Finally, the pure protein was dialyzed against 100 mM KH_2PO_4, pH 7, with 30 mM EDTA and then several times against buffer alone.

The protein was characterized by SDS−PAGE and electrospray mass spectrometry (ES/MS). Mass spectral measurements were performed at the University of Illinois mass spectroscopy laboratory. The observed molecular weight (17 347.6) corresponds to the calculated molecular weight (17 345.1) of the mutant protein of swMb(L29H,F43H) within experimental error.

UV−Vis Characterization. A Cary 3E double-beam UV−vis spectrometer was used to monitor the changes in the UV−vis spectrum of Cu_BMb associated with Cu(II) binding. The titrations were performed at 20 °C using 1750 μL of ∼8 μM protein in 20 mM Tris pH 8.2 and the same volume of buffer in the reference cuvette. Aliquots of Cu(II) were added to both the protein and the reference cuvette. The data were plotted by the double reciprocal plot method[55,57] and fit to the equation

$$1/\Delta A = (K_D/\Delta A_{inf})(1/[M]) + 1/\Delta A_{inf}$$

where ΔA is the difference between maximum and minimum absorption, [M] is the concentration of free metal ions, which is assumed to be equal to the total concentration of added metal ions, and ΔA_{inf} is the absorbance change for the complete formation of the adduct.

A Hewlett-Packard 8453 UV−vis spectrometer, equipped with a circulating water bath and a Polyscience digital temperature controller, was used to monitor the binding of cyanide to Cu_BMb. For cyanide binding, KCN was added to 1 mL of ∼5 μM protein in 100 mM KH_2PO_4, pH 7, with stirring. Aliquots of 100 μL were removed immediately after each addition of KCN and stored in a microfuge tube. Identical experiments were performed using 1−2 equiv of either $Cu^{II}SO_4$ or $Zn^{II}SO_4$. UV−vis measurements were taken after the samples were incubated for 6 h. This procedure ensured that CN binding was complete. All measurements were performed at 20 °C. After corrections for dilution were made, the data were plotted by the double reciprocal plot method described above.

UV−vis was also used to monitor the reduced and oxy forms of the protein. Manipulation of the reduced protein in the absence of air was performed in a glovebox under an argon atmosphere. O_2 was removed from all solvents and the protein by three consecutive trials of the freeze−pump−thaw technique on a Schlenk line and then transferred to the glovebox. The protein was reduced with dithionite and passed down a PD10 column equilibrated with 20 mM Tris, pH 8.2, to remove the excess reductant. The sample was then transferred to an airtight cuvette with a sidearm which contained either tetrakis(acetonitrile)-Cu(I) hexafluorophosphate or Ag^INO_3. UV−vis measurements on the sample were then taken before and after the contents in the sidearm were mixed with the protein.

The effect of Ag(I), as a mimic for Cu(I), on O_2 binding to the Cu_B-Mb was followed by UV−vis spectroscopy. Addition of Ag(I) to the reduced protein was performed in 20 mM Tris, pH 8.2, using 2 mL of ∼6 μM protein in a 3-mL cuvette. To avoid precipitation of Ag(I), the pH of the buffer was adjusted with H_2SO_4 instead of HCl.

Elemental Analysis. The content of iron, copper, and zinc ions in Cu_BMb and the CN^- adduct of the protein was determined by elemental analysis using inductively coupled plasma atomic emission spectrometry conducted at the School of Chemical Sciences Microanalysis Laboratory at the University of Illinois. The samples were prepared by adding a slight excess of Cu(II) to 200 μL of the 0.8 mM protein sample. Free Cu(II) was removed by passing the protein down a PD10 column.

EPR Characterization. EPR spectra were recorded on a Bruker ESP 300 equipped with an Oxford liquid helium cryostat and an ITC4 temperature controller. Samples were prepared at room temperature by slow addition of $CuSO_4$ to the protein in 100 mM KH_2PO_4, pH 7, with 25% glycerol with stirring. The samples were then flash frozen in liquid nitrogen. The final volume and concentration of each EPR sample was 200 μL and 0.6−0.9 mM. The molar extinction coefficient, calculated using the standard hemochromagen method,[58,59] of the Soret transition at 408 nm (151.2 mM^{-1}) for Cu_BMb was used to determine protein concentrations.

Results and Discussion

Design of the Cu_B Center into Sperm Whale Myoglobin. An overlay of the Cu_B-heme active site of bovine C*c*O with the active site of swMb(L29H, F43H) (called Cu_BMb) is shown in Figure 1a. The mutations of distal swMb residues were chosen on the basis of their overall position relative to the native ligands and also the position of the Cu(II) relative to the heme. In the swMb model, the heme overlays quite well with the heme of the native enzyme. Thus, the Cu(II) ion in the swMb model occupies a similar position with respect to the heme as in the native protein. Figure 1b shows an overlay of the native swMb with swMb(L29H, F43H). This view demonstrates that only minor rotations of the side chains are required to allow binding of copper. The energy parameters for WTswMb, after minimization (as a control), and those of the Cu_BMb match well (see Table 1). The bond lengths between Cu(II), the three histidine ligands, and the heme of C*c*O from bovine heart, *P. denitrificans*, and the swMb mutant are compared in Table 2. The similarity of the binding-site parameters observed between Cu_B-Mb and native C*c*O suggests that these mutations may allow formation of a heme-copper center in Mb.

UV−Vis Spectral Characterization. The UV−vis spectra of Cu_BMb in the pH range from 7 to 8.2 are similar to that observed for WTswMb[41] and are typical of a six-coordinate, H_2O-bound, high-spin heme with an intense Soret band at 408 nm (ϵ = 151.2 mM^{-1}) and a charge-transfer band at 628 nm (Figure 2). Thus, the double mutation does not significantly

(56) Kachalova, G. S.; Popov, A. N.; Bartunik, H. D. *Science (Washington, D.C.)* **1999**, *284*, 473.
(57) Wariishi, H.; Valli, K.; Gold, M. H. *J. Biol. Chem.* **1992**, *267*, 23688.
(58) De Duve, C. *Acta Chem. Scand.* **1948**, *2*, 264.
(59) Morrison, M.; Horie, S. *Anal. Biochem.* **1965**, *12*, 77.

Table 1. Energy Parameters for Native Sperm Whale Mb before (WTswMb) and after (WTswMb(min)) 1000 Steps of Minimization and Cu_BMb after 1000 Steps of Minimization

	WTswMb	WTswMb(min)	Cu_BMb
bond energy	417.2901	59.8795	62.7291
angle energy	646.6017	337.7403	329.9886
dihedral energy	356.2208	340.9347	356.3217
improper energy	171.5280	27.9041	31.0115
Lennard-Jones energy	3 152.9866	−1 392.4301	−1 310.7236
electrostatic energy	−7 734.7056	−10 443.6475	−9 613.9541
constraints, other	0.0005	0.0000	0.0000
total CHARMm energy	−2 990.0784	−11 069.6182	−10 144.6292

Table 2. Comparison of Bond Lengths (Å) of the Cu_B Sites in Native C*c*O and in Cu_BMb

	bovine C*c*O	*P. denitrificans* C*c*O	Cu_BMb
bond length			
His A−Cu	1.850	1.969	2.032
His B−Cu	2.159	2.033	2.270
His C−Cu	2.153	2.114	2.415
Cu−Fe distance	4.695	5.345	5.364

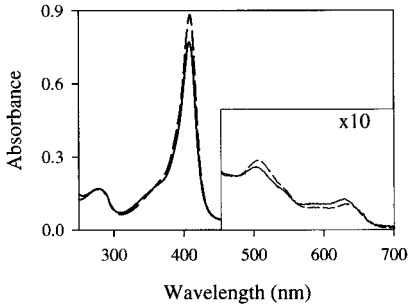

Figure 2. UV−vis spectra of high-spin ferric WTswMb (solid line) and Cu_BMb (dashed line). Spectra were recorded with the samples in 100 mM KH_2PO_4, pH 7, at 20 °C.

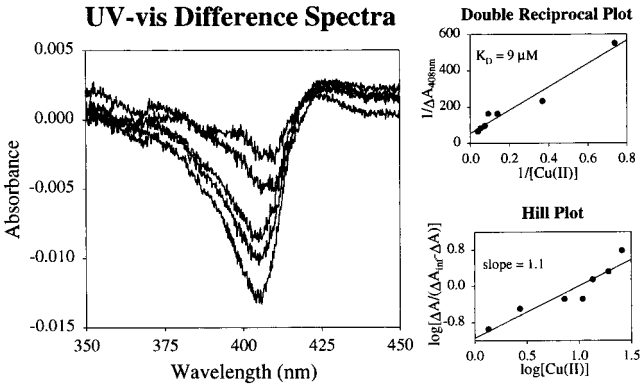

Figure 3. UV−vis difference spectra of Cu(II) binding to Cu_BMb. (Inset, top) Double reciprocal plot of the change in Cu(II) concentration versus the change in absorbance. (Inset, bottom) Hill plot of the data. Spectra were recorded at 20 °C with the sample in 20 mM Tris, pH 8.2.

perturb the structure of the protein. Addition of Cu(II) at pH 8.2 to Cu_BMb resulted in a difference spectrum (Figure 3a), whose changes in the Soret region were fit to a double reciprocal plot (Figure 3b) and a Hill plot (Figure 3c, slope = 1.12). These results indicate that a single copper-binding site with a K_D of 9 μM was created in Cu_BMb.

One of the characteristics of heme-copper oxidases is the spin-coupled Cu(II) and heme Fe(III) center bridged by a ligand such as cyanide.[2−6] Therefore, the cyanide derivatives of Cu_BMb in the presence or absence of Cu(II) were studied further by UV−vis absorption spectroscopy. Binding of CN^- to Cu_BMb caused

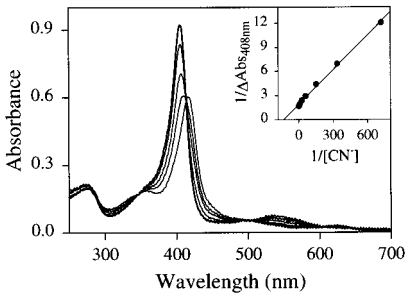

Figure 4. UV−vis spectra following the binding of CN^- to Cu_BMb. (Inset) Double reciprocal plot of the change in CN^- concentration versus the change in absorbance between 425 and 407 nm. Spectra were recorded in 100 mM KH_2PO_4, pH 7, at 20 °C.

UV−vis spectral changes characteristic of a shift from high- to low-spin heme, with the largest changes at 407 and 425 nm (Figure 4). It was observed that fewer equivalents of CN^- were needed to cause the same spectral changes when Cu(II) was present. Therefore, the binding affinity of Cu_BMb for CN^- without Cu(II) was compared to the affinity of Cu_BMb in the presence of 2 equiv of Cu(II). Double reciprocal plots of the changes in absorption at 407 and 425 nm upon the addition of CN^- were plotted against the change in CN^- concentration (Figure 4 inset). From the resulting plots the binding affinity for CN^- was obtained. Interestingly, Cu_BMb exhibited a 20-fold increase in its binding affinity for CN^- in the presence of 2 equiv of Cu(II) (K_b = 7.1 mM^{-1} without Cu(II) compared to K_b = 143.9 mM^{-1} with Cu(II)). This result is consistent with a model in which CN^- interacts with both Fe(III) and Cu(II), probably bridging the two metal centers. Similar experiments were performed using 2 equiv of Zn(II). Once again, the affinity for CN^- was increased by the addition of Zn(II) (K_b = 60 mM^{-1}), although to a lesser extent than that for Cu(II).

Elemental Analysis. Additional evidence for CN^- bridging between Fe(III) and Cu(II) in Cu_BMb comes from the elemental analysis results. When excess Cu(II) was added to the high-spin Cu_BMb and passed down a size exclusion column to remove free Cu(II) ions, the content of Fe(III) and Cu(II) in this sample was found to be 10.8 and 0.2 μM, respectively. This result suggests that Cu(II) binds only weakly to Cu_BMb and is removed upon size exclusion chromatography. However, when the experiment was repeated with 1.2 equiv of CN^- and 1.2 equiv of Cu(II), the concentrations of Fe(III) and Cu(II) after the sample was passed down a size exclusion column were found to be 17.7 and 17.3 μM. Thus, a 1:1 ratio of heme Fe to Cu was obtained in the Cu_BMb-CN^- derivative. The same experiment was also performed using Zn(II) in place of Cu(II). In this case the final concentrations of Fe and Zn after the sample was passed down the size exclusion column were 19.8 and 15.1 μM. Thus, Zn(II) binds to Cu_BMb-CN^- with a slightly lower affinity than that of Cu(II). This observation is consistent with the results obtained by UV−vis spectroscopy presented above.

EPR Characterization. The proposal of a bridged structure for Cu(II)-CN-heme in Cu_BMb is further supported by EPR results (see Figure 5). The spectrum of the sample before Cu(II) was added exhibited mostly low-spin heme signals at g = 3.35, 2.06 with a minor signal at g = 6.06 due to a cyanide-free heme species. After addition of 0.5 equiv of Cu(II), the intensity of all low-spin heme signals decreased by approximately half. After the addition of another 0.88 equiv (1.38 equiv total) of Cu(II), the heme signals disappeared completely and a Cu(II) signal appeared due to the slight excess of Cu(II). The disappearance of the heme signal indicated the heme Fe(III) and the Cu(II) antiferromagnetically couple as observed

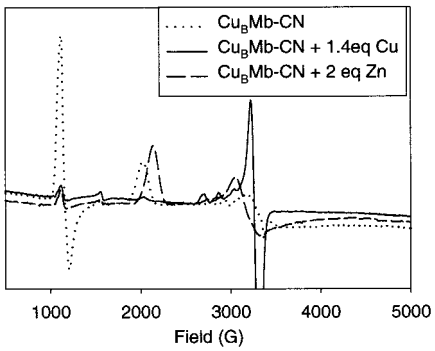

Figure 5. X-band EPR spectra of 0.6 mM Cu_BMb-CN before (dotted line) and after the addition of 0.72 mM $Cu^{II}SO_4$ (solid line) and 1.2 mM $Zn^{II}SO_4$ (dashed line). Samples were recorded in 100 mM KH_2PO_4, pH 7, at 20 K and 5 mW power.

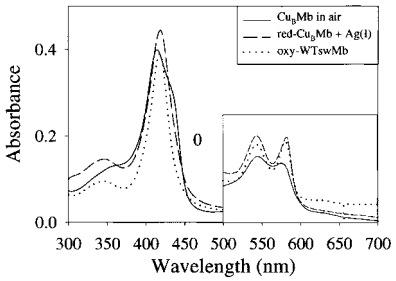

Figure 6. UV−vis spectra of reduced Cu_BMb in air (solid line), reduced Cu_BMb in air after the addition of Ag(I)NO_3 (dashed line), and reduced WTswMb in air (dotted line). Spectra were recorded in 20 mM Tris·NO_3, pH 8.2, at 20 °C.

for the CN^- adducts of native HCO enzymes. Furthermore, no decrease in the heme signal was observed after the addition of Cu(II) to the CN^- adduct of WTMb. This evidence strongly supports Cu(II) binding to the designed site and formation of a heme-Fe(III)-CN-Cu(II) bridge in this system.

The EPR spectra after addition of Zn(II) to the CN-bound protein further support these conclusions. The spectra of the Cu_BMb-CN before and after the addition of Zn(II) are shown in Figure 5. After the addition of Zn(II) to the sample, the positions of the low-spin signals shift to $g = 3.17$ and 2.13 but clearly still represent a low-spin CN-bound heme. This result indicates that the interaction of Zn(II) with CN^- caused a minor change in the heme environment but did not displace the CN^-. Furthermore, the minor high-spin heme signal at $g = 6$ disappeared completely after the addition of Zn(II), concurrent with the shift in position and increase in the signal intensity of the low-spin signal. This observation can be explained by an increase in the affinity of the protein for CN^- in the presence of Zn(II) and is consistent with the results in the UV−vis study presented above. These results suggest that Zn(II) binds to the designed Cu_B site of Cu_BMb-CN^- in a similar fashion as in Cu(II)-bound Cu_BMb-CN^-. No decrease of the dominant low-spin EPR signals in Zn(II)-bound Cu_BMb-CN^- occurs because no unpaired electron is available in Zn(II) for spin coupling with heme Fe(III).

O_2 Binding. As an efficient O_2 carrier, WTswMb binds O_2 reversibly. The creation of a Cu_B binding site in swMb presents us with an excellent opportunity to investigate the effect of copper ions on the ability of Mb to bind O_2. Exposure of the Cu(II)-free reduced Cu_BMb to air (Figure 6) resulted in partial binding of O_2 as indicated by the resulting UV−vis spectrum, which has a Soret peak at 418 nm (oxy Cu_BMb) with a shoulder at 434 nm (reduced five-coordinate Cu_BMb). The mutations in the distal pocket apparently reduced the O_2-binding affinity of the protein below that of the WT swMb. However, when aliquots of Ag(I), as a Cu(I) mimic, were added to the protein, a clear decrease in the shoulder at 434 nm is observed along with an increase in the band at 418 nm. The final spectrum (Figure 6) is identical to that of oxy WTMb. This can be explained by an increased affinity for O_2 when Ag(I) binds to the site.

In summary, we have shown that it is possible to design and engineer metal-binding sites in proteins on the basis of the active sites of proteins with little sequence and structural homology. This principle has been demonstrated by creating a Cu(II)-binding site next to the heme center in sperm whale myoglobin after a careful structural comparison and modeling. Evidence from UV−vis, elemental analysis, and EPR studies of both resting state and CN^- derivatives of the engineered Cu_BMb support the conclusion that a heme-copper center is created in swMb. The presence of copper ions in the designed Cu_B center in swMb increased its affinity for diatomic ligands such as CN^- and O_2. Further study is being carried out to provide insight into the structure and function of this model heme-copper center.

Acknowledgment. We thank Professor Stephen G. Sligar for the gift of the sperm whale myoglobin gene, and Professor Robert B. Gennis for helpful discussions. This material is based on work supported by the National Science Foundation under Award No. CHE 95-02421 to Y.L. (CAREER Award and Special Creativity Extension). Y.L. is a Sloan Research Fellow of the Alfred Sloan Foundation, a Cottrell Scholar of the Research Corporation, a Camille Dreyfus Teacher-Scholar of the Camille and Henry Dreyfus Foundation, and a Beckman Young Investigator of the Arnold and Mabel Beckman Foundation.

JA0015343